Combining the Semiclassical Initial Value Representation with Centroid Dynamics†

Being J. Ka and Gregory A. Voth*

Department of Chemistry and Henry Eyring Center for Theoretical Chemistry, University of Utah, Salt Lake City, Utah 84112-0850

Received: December 14, 2003; In Final Form: February 13, 2004

A semiclassical initial value representation (SC-IVR) for centroid dynamics (CD) is derived to provide a more accurate description of quantum time correlation functions (TCFs). The time-dependent quasi-density operator (QDO) in SC-IVR-CD is shown to exhibit more exact behavior than that of the CMD approximation, thereby improving the calculated quantum TCFs. Three typical one-dimensional model potentials (weak anharmonic, double well, and quartic) were studied as examples in calculating TCFs with the SC-IVR-CD method. Importantly, for intermediate temperatures, SC-IVR-CD gives a more exact description of the coherent behavior of the quantum TCFs than does centroid molecular dynamics (CMD).

I. Introduction

The calculation of quantum time correlation functions (TCFs) is an intriguing and very challenging subject in chemical physics. In principle, exact quantum TCFs are obtained using both exact quantum thermal distributions and exact quantum time propagation schemes. Exact quantum thermal distributions can be obtained from path integral techniques.[1] Exact quantum time propagation, in principle, can be achieved from propagating wave functions to solve the time-dependent Schrödinger equation (wave packet dynamics) or from propagating the density operator to solve the Heisenberg equation (the quantum Liouville equation). It is well-known that these latter approaches are not practical using any existing computational tools except for low-dimensional systems. Moreover, the requirement that the quantum propagation should be averaged over a quantum thermal distribution function further complicates the problem.

There are, however, several approximate techniques developed by a number of researchers for the calculation of quantum TCFs. One possible approach is to use the semiclassical initial value representation (SC-IVR) to propagate trajectories which are sampled from equilibrium distributions.[2−9] For example, Wang et al.[10] have calculated the flux-side correlation function to get the reaction rate for a reaction coordinate coupled to a harmonic bath. Using another approach, Krilov et al.[11] have combined real-time PIMC with maximum entropy methods (MaxEnt)[12] for calculating symmetrized time correlation functions. Centroid molecular dynamics (CMD)[13,14] is another approach with which one can calculate approximate time correlation functions.

In this paper, the exact theory of centroid dynamics (CD)[15] is combined with the SC-IVR method. In principle, exact CD can give exact TCFs, although the numerical cost and scaling with system size would be prohibitive. However, SC-IVR has been shown to capture important interference effects that are not well-described by CMD,[14] so this fact provides the motivation to develop a CD formulation using SC-IVR.

The present paper is organized as follows: In section II, the basic combination of SC-IVR with CD is described (called SC-IVR-CD). Then, in section III results from this combined formalism are presented. Concluding remarks are given in section IV.

II. Theory

In this section, the key features of CD are first briefly reviewed in section II.A., while the SC-IVR representation of CD is introduced in section II.B.

II.A. Exact Centroid Variables and the CMD Approximation. A general quantum time correlation function between operator $\hat{A}$ and $\hat{B}$, can be defined as[15]

$$C_{AB}^{\mathrm{qm}}(t) \equiv \frac{1}{Z}\mathrm{Tr}[\mathrm{e}^{-\beta\hat{H}}\hat{A}\mathrm{e}^{\mathrm{i}\hat{H}t/\hbar}\hat{B}\mathrm{e}^{-\mathrm{i}\hat{H}t/\hbar}] = \langle A(0)B(t)\rangle \qquad (1)$$

where Z is the partition function, given by $\mathrm{Tr}[\mathrm{e}^{-\beta\hat{H}}]$. This correlation function is related to the CD time correlation function, $C_{AB}^{\mathrm{CD}}(t)$ defined below in eq 4, through the Fourier transform relationship

$$\tilde{C}_{AB}^{\mathrm{qm}}(\omega) = \frac{\hbar\beta\omega}{2}\left[\coth\left(\frac{\hbar\beta\omega}{2}\right) + 1\right]\tilde{C}_{AB}^{\mathrm{CD}}(\omega) \qquad (2)$$

This relationship holds as long as $\hat{A}$ is a linear operator of the form[15]

$$\hat{A} = A_0 + A_1\hat{x} + A_2\hat{p} \qquad (3)$$

Time correlation functions are expressed in centroid dynamics as the following equations which employ a time-dependent quasi-density operator (TD-QDO)[15] as a key component. The CD TCFs are given by

$$C_{AB}^{\mathrm{CD}}(t) \equiv \frac{1}{Z}\int\int\frac{\mathrm{d}x_{\mathrm{c}}\,\mathrm{d}p_{\mathrm{c}}}{2\pi\hbar}\rho_{\mathrm{c}}(x_{\mathrm{c}},p_{\mathrm{c}})A_{\mathrm{c}}B_{\mathrm{c}}(t) \qquad (4)$$

where

$$B_{\mathrm{c}}(t) = \mathrm{Tr}[\mathrm{e}^{-\mathrm{i}\hat{H}t/\hbar}\hat{\delta}_{\mathrm{c}}(x_{\mathrm{c}},p_{\mathrm{c}})\mathrm{e}^{\mathrm{i}\hat{H}t/\hbar}\hat{B}] \qquad (5)$$

and x_{c} and p_{c} are the position and momentum centroid, respectively. It should be noted that all formulas in this paper are given for a one-dimensional problem, but they can be readily

† Part of the special issue "Hans C. Andersen Festschrift".

10.1021/jp037862h CCC: $27.50
Published on Web 04/06/2004

generalized. In eq 4 above $\rho_c(x_c,p_c)$ is the equilibrium centroid density, given by

$$\rho_c(x_c,p_c) = e^{-\beta p_c^2/2m}\rho_c(x_c) \tag{6}$$

$$\rho_c(x_c) = \mathrm{Tr}[\hat{\varphi}(x_c)] \tag{7}$$

where $\hat{\varphi}(x_c)$ is defined in eq 10 below. The TD-QDO is given by

$$\hat{\delta}_c(t;x_c,p_c) \equiv e^{-i\hat{H}t/\hbar}\hat{\delta}_c(x_c,p_c)e^{i\hat{H}t/\hbar} \tag{8}$$

with the matrix elements of the initial QDO $\hat{\delta}_c(x_c,p_c)$ given by

$$\langle x'|\hat{\delta}_c(x_c,p_c)|x''\rangle = \frac{e^{ip_c(x'-x'')/\hbar}}{e^{-m(x'-x'')2/2\beta\hbar^2}}\frac{\langle x'|\varphi(x_c)|x''\rangle}{\rho_c(x_c)} \tag{9}$$

where

$$\langle x'|\hat{\varphi}(x_c)|x''\rangle = \sqrt{\frac{2\pi\hbar^2\beta}{m}}\lim_{P\to\infty}\left(\frac{mP}{2\pi\hbar^2\beta}\right)^{P/2}\int dx_2 \cdots \int dx_P \delta(x_c - x_0) \times \exp\left\{-\frac{mP}{2\hbar^2\beta}[(x'-x_2)^2 + \cdots + (x_P - x'')^2] - \frac{\beta}{P}\left[\frac{1}{2}V(x') + V(x_2) + \cdots + \frac{1}{2}V(x'')\right]\right\} \tag{10}$$

The exact TD-QDO is the solution of the following quantum Liouville equation:[15]

$$\frac{d}{dt}\hat{\delta}_c(t;x_c,p_c) = -\frac{i}{\hbar}[\hat{H},\hat{\delta}_c(t;x_c,p_c)] \tag{11}$$

The numerical matrix multiplication (NMM) method[16] can be used to get the exact solution of eq 11 for the TD-QDO of low-dimensional systems. However, as might be expected, solving eq 11 for many degrees of freedom is not possible using this or any other numerically exact approach. It is also formidable to calculate correlation functions in which one needs to average this quantity over many initial position and momentum centroid samplings. Therefore, instead of propagating the QDO by eq 11 exactly, it is desirable to obtain approximate expressions for the TD-QDO in eq 8, to derive new relationships between eq 4 or eq 5, and a new approximate TD-QDO. One older example of such an approximation is of course the CMD formalism,[14] which employs the following key approximation:

$$\hat{\delta}_c(t;x_c,p_c) \approx \hat{\delta}_c(x_c(t),p_c(t)) \tag{12}$$

The CMD method is very practical, but its validity is primarily limited to incoherent dynamics.[15] While most interesting condensed phase systems are in the incoherent limit, there are important cases where coherent motion is important (e.g., weakly damped anharmonic molecular vibrations).

II.B. Semiclassical Initial Value Representation (SC-IVR) of Centroid Dynamics. To derive semiclassical representations of centroid variables, one needs to first find a semiclassical representation of the TD-QDO. This is described below in section II.B.1. Some fundamental relationships are then derived in section II.B.2 and section II.B.3. It is also appropriate to mention the forward−backward approximation of SC-IVR.[17−20] FB-IVR has been suggested to achieve faster convergence when the operator, for example, $\hat{B}$ of eq 4, is expressed as an exponential. Then pairs of evolution operators along with the operator of interest can be combined into a single-exponential operator, resulting in increased computational efficiency. However, the additional stationary phase approximation which is employed in FB-IVR may not describe the coherence properly, while SC-IVR retains such behavior. For a detailed analysis of this issue, the reader is referred to the work of Thoss et. al. (especially Figure 4).[9] Therefore, full SC-IVR is chosen for this work, and the subsequent sections employ only this approach in the SC-IVR formulation of CD.

II.B.1. SC-IVR Formulation of the Time-Dependent Quasi-Density Operator (TD-QDO). The Herman−Kluk[21] version of SC-IVR amounts to the following approximation for the quantum mechanical time evolution operator:

$$e^{-i\hat{H}t/\hbar} \approx (2\pi\hbar)^{-1}\int\int dp_0\, dx_0 C_t(p_0,x_0)e^{[iS_t(p_0,x_0)/\hbar]}|p_t x_t\rangle\langle p_0 x_0| \tag{13}$$

where $\langle x|p_t x_t\rangle = (\gamma/\pi)^{1/4}\exp[-(\gamma/2)(x - x_t)^2 + (i/\hbar)p_t(x - x_t)]$ constitutes a semiclassical coherent state basis. By inserting eq 13 into eq 8 twice, the SC-IVR expression of the TD-QDO becomes[20]

$$\begin{aligned}\langle x'|\hat{\delta}_c(t;x_c,p_c)|x''\rangle &= \langle x'|e^{-i\hat{H}t/\hbar}\hat{\delta}_c(x_c,p_c)e^{i\hat{H}t/\hbar}|x''\rangle \\ &\approx (2\pi\hbar)^{-2}\int\int dp_0\, dx_0 \int\int \times \\ &\quad dp'_0\, dx'_0\, C_t(p_0,x_0)C_t(p'_0,x'_0)^* \times \\ &\quad e^{(i/\hbar)[S_t(p_0,x_0)-S_t(p'_0,x'_0)]} \times \\ &\quad \langle p_0 x_0|\hat{\delta}_c(x_c,p_c)|p'_0 x'_0\rangle\langle p'_t x'_t|x''\rangle\langle x'|p_t x_t\rangle \\ &\equiv \langle x'|\hat{\delta}_c^{sc}(t;x_c,p_c)|x''\rangle\end{aligned} \tag{14}$$

The last line of eq 14 defines the SC-IVR representation of the TD-QDO which is used in the subsequent derivations. However, each component of eq 14 needs to first be discussed in more detail.

The term $\langle p_0 x_0|\hat{\delta}_c(x_c,p_c)|p'_0 x'_0\rangle$ in eq 14 connects the sampling of the semiclassical coherent state basis to the initial QDO through the following relationship:

$$\langle p_0 x_0|\hat{\delta}_c(x_c,p_c)|p'_0 x'_0\rangle = \int\int dx'\, dx''\, \langle p_0 x_0|x'\rangle\langle x'|\hat{\delta}_c(x_c,p_c)|x''\rangle\langle x''|p'_0 x'_0\rangle \tag{15}$$

The initial QDO of eq 14 is given by eqs 9 and 10. The other parts of eq 14, such as the prefactor, action, and overlap between coherent state basis of SC-IVR, are given, respectively, by

$$C_t(p_0,x_0) = \sqrt{\det\left[\frac{1}{2}\left(\frac{\partial p_t}{\partial p_0} + \frac{\partial x_t}{\partial x_0} - i\gamma\hbar\frac{\partial x_t}{\partial p_0} + \frac{i}{\gamma\hbar}\frac{\partial p_t}{\partial x_0}\right)\right]} \tag{16}$$

$$S_t(p_0,x_0) = \int_0^t dt'\, L(p_{t'},x_{t'}) \tag{17}$$

where L is Lagrangian, and

$$\langle p'_t x'_t|x''\rangle\langle x'|p_t x_t\rangle = \left(\frac{\gamma}{\pi}\right)^{1/4}\exp\left[-\frac{\gamma}{2}(x'' - x'_t)^2 - \frac{i}{\hbar}p'_t(x'' - x'_t)\right]\left(\frac{\gamma}{\pi}\right)^{1/4}\exp\left[-\frac{\gamma}{2}(x' - x_t)^2 + \frac{i}{\hbar}p_t(x' - x_t)\right] \tag{18}$$

This quantity can be re-expressed as

$$\langle p'_t x'_t|x''\rangle\langle x'|p_t x_t\rangle = \sqrt{\frac{\gamma}{\pi}}\exp\left[-\gamma\left(\bar{x}-\frac{x_t+x'_t}{2}\right)^2+\frac{i}{\hbar}(p_t-p'_t)\left(\bar{x}-\frac{x_t+x'_t}{2}\right)\right]\exp\left[-\gamma\left(\frac{\Delta x}{2}-\frac{x_t-x'_t}{2}\right)^2+\frac{i}{\hbar}(p_t+p'_t)\left(\frac{\Delta x}{2}-\frac{x_t-x'_t}{2}\right)\right] \quad (19)$$

where $\bar{x} \equiv (x' + x'')/2$ and $\Delta x \equiv x' - x''$.

If the QDO itself is the quantity of interest, which is the case in some of the numerical examples below, one can calculate eq 14 numerically, the details of which are included in section III.

II.B.2 SC-IVR of Centroid Position-Dependent Variables. Equation 4 necessitates the determination of the SC-IVR time-dependent centroid variable, eq 5, given by

$$B_c^{sc}(t) \equiv \mathrm{Tr}[\hat{\delta}_c^{sc}(t;x_c,p_c)\hat{B}] \quad (20)$$

for an arbitrary operator $\hat{B}$. If this operator involves of the position operator, $\hat{x}$, that is, $\hat{B} = B(\hat{x})$, its SC-IVR expression is obtained, using eq 14, as

$$B_c^{sc}(t) = \int dx\langle x|\hat{\delta}_c^{sc}(t;x_c,p_c)|x\rangle B(x) \quad (21)$$

$$= (2\pi\hbar)^{-2}\int\int dp_0\,dx_0\int\int dp'_0\,dx'_0\,C_t(p_0,x_0)C_t(p'_0,x'_0)^*\times e^{(i/\hbar)[S_t(p_0,x_0)-S_t(p'_0,x'_0)]}\langle p_0x_0|\hat{\delta}_c(x_c,p_c)|p'_0x'_0\rangle\times\langle p'_tx'_t|B(\hat{x})|p_tx_t\rangle \quad (22)$$

A change of integration order was made between eq 21 and eq 22. The term in eq 22 satisfies eq 23 below, and this is used for the derivation of eqs 24, 33, and 34 later, such that

$$\langle p'_tx'_t|B(\hat{x})|p_tx_t\rangle = \mathrm{Tr}[|p_tx_t\rangle\langle p'_tx'|B(\hat{x})] = \int dx\,\langle p'_tx'_t|x\rangle\langle x|p_tx_t\rangle B(x) \quad (23)$$

To get the SC-IVR time-dependent position centroid variable, for example, one substitutes $B(\hat{x}) = \hat{x}$ into eq 22 and uses the equation

$$\langle p'_tx'_t|\hat{x}|p_tx_t\rangle = \int dx\,\langle p'_tx'_t|x\rangle\langle x|p_tx_t\rangle x \quad (24a)$$

$$= \frac{(x'_t+x_t)+i\gamma^{-1}\hbar^{-1}(p_t-p'_t)}{2}\times\exp\left[-\frac{\gamma(x_t-x'_t)^2}{4}-\frac{(p_t-p'_t)^2}{4\gamma\hbar^2}-\frac{i}{2\hbar}(x_t-x'_t)(p_t+p'_t)\right] \quad (24b)$$

$$\equiv x_{sc}(p'_tx'_tp_tx_t)\langle p'_tx'_t|p_tx_t\rangle \quad (24c)$$

where two terms in eq 24c are defined as the prefactor and exponential of eq 24b, respectively. The SC-IVR-CD definition of the centroid variable, $x_c^{sc}(t)$, now reads

$$x_c^{sc}(t) = (2\pi\hbar)^{-2}\int\int dp_0\,dx_0\int\int dp'_0\,dx'_0\,C_t(p_0,x_0)C_t(p'_0,x'_0)^*\times e^{(i/\hbar)[S_t(p_0,x_0)-S_t(p'_0,x'_0)]}\langle p_0x_0|\hat{\delta}_c(x_c,p_c)|p'_0x'_0\rangle\times x_{sc}(p'_tx'_tp_tx_t)\langle p'_tx'_t|p_tx_t\rangle \quad (25)$$

In order to write long expressions in a compact form, we introduce the following integral notations which will appear frequently from now on.

$$d\Gamma \equiv dx_0\,dp_0/(2\pi\hbar) \quad (26)$$

$$\int^{SC} d\Gamma\,d\Gamma'\{\cdots\} \equiv \int d\Gamma\,d\Gamma'\,C_t(p_0,x_0)C_t(p'_0,x'_0)^* e^{\frac{i}{\hbar}[S_t(p_0,x_0)-S_t(p'_0,x'_0)]}\{\cdots\} \quad (27)$$

$$\int^{SCCD} d\Gamma\,d\Gamma'\,\{\cdots\} \equiv \int^{SC} d\Gamma\,d\Gamma'\,\langle p_0x_0|\hat{\delta}_c(x_c,p_c)|p'_0x'_0\rangle\langle p'_tx'_t|p_tx_t\rangle\{\cdots\} \quad (28)$$

Then the SC-IVR expression of an arbitrary centroid variable is thus simplified as

$$B_c^{sc}(t) = (2\pi\hbar)^{-2}\int\int dp_0\,dx_0\int\int dp'_0\,dx'_0\,C_t(p_0,x_0)C_t(p'_0,x'_0)^* e^{(i/\hbar)[S_t(p_0,x_0)-S_t(p'_0,x'_0)]}\times\langle p_0x_0|\hat{\delta}_c(x_c,p_c)|p'_0x'_0\rangle B_{sc}(p'_tx'_tp_tx_t)\langle p'_tx'_t|p_tx_t\rangle$$

$$= \int^{SC} d\Gamma\,d\Gamma'\langle p_0x_0|\hat{\delta}_c(x_c,p_c)|p'_0x'_0\rangle B_{sc}(p'_tx'_tp_tx_t)\times\langle p'_tx'_t|p_tx_t\rangle$$

$$= \int^{SCCD} d\Gamma\,d\Gamma'\,B_{sc}(p'_tx'_tp_tx_t) \quad (29)$$

with the definition of

$$B_{sc}(p'_tx'_tp_tx_t) \equiv \mathrm{Tr}[|p_tx_t\rangle\langle p'_tx'_t|B(\hat{x})]/\mathrm{Tr}[|p_tx_t\rangle\langle p'_tx'_t|] \quad (30)$$

The above convention satisfies

$$\int^{SCCD} d\Gamma\,d\Gamma' = \int^{SC} d\Gamma\,d\Gamma'\,\langle p_0x_0|\hat{\delta}_c(x_c,p_c)|p'_0x'_0\rangle\langle p'_tx'_t|p_tx_t\rangle \simeq 1 \quad (31)$$

by the normalization condition, $\mathrm{Tr}[\hat{\delta}_c^{sc}(t;x_c,p_c)] = \int dx\,\langle x|\hat{\delta}_c^{sc}(t;x_c,p_c)|x\rangle \simeq 1$ of eq 14.

With the conventions of eqs 26−28, eq 25 simply reads as

$$x_c^{sc}(t) \equiv \int^{SCCD} d\Gamma\,d\Gamma'\,x_{sc}(p'_tx'_tp_tx_t) \quad (32)$$

Other SC-IVR-CD expressions are given by

$$V_c^{sc}(t) = \int dx\,\langle x|\hat{\delta}_c^{sc}(t;x_c,p_c)|x\rangle V(x) = \int^{SC} d\Gamma\,d\Gamma'\,\langle p_0x_0|\hat{\delta}_c(x_c,p_c)|p'_0x'_0\rangle[\int dx\,\langle p'_tx'_t|x\rangle\times\langle x|p_tx_t\rangle V(x)]$$

$$= \int^{SCCD} d\Gamma\,d\Gamma'\,V_{sc}(p'_tx'_tp_tx_t) \quad (33)$$

$$F_c^{sc}(t) = \int dx\,\langle x|\hat{\delta}_c^{sc}(t;x_c,p_c)|x\rangle\left[-\frac{dV(x)}{dx}\right] \quad (34a)$$

$$= \int^{SC} d\Gamma\,d\Gamma'\,\langle p_0x_0|\hat{\delta}_c(x_c,p_c)|p'_0x'_0\rangle[\int dx\,\langle p'_tx'_t|x\rangle\times\langle x|p_tx_t\rangle F(x)] \quad (34b)$$

$$= \int^{SCCD} d\Gamma\,d\Gamma'\,F_{sc}(p'_tx'_tp_tx_t) \quad (34c)$$

where eq 30 defines the following equations:

$$V_{sc}(p'_tx'_tp_tx_t) = (\int dx\,\langle p'_tx'_t|x\rangle\langle x|p_tx_t\rangle V(x))/\langle p'_tx'_t|p_tx_t\rangle \quad (35)$$

$$F_{sc}(p'_t x'_t p_t x_t) = \left(\int dx \langle p'_t x'_t|x\rangle\langle x|p_t x_t\rangle F(x)\right)/\langle p'_t x'_t|p_t x_t\rangle \quad (36)$$

It should be noted that integrations in eqs 35 and 36 are done analytically in some cases.

II.B.3 SC-IVR of Momentum-Dependent Centroid Variables. The SC-IVR expressions for the momentum and kinetic energy centroid variables require the differential expressions of the QDO. To obtain such expressions, one uses eqs 14 and 19 to get the following expressions:

$$\left[\frac{\partial}{\partial \Delta x}\langle x'|\hat{\delta}_c^{sc}(t;x_c,p_c)|x''\rangle\right]_{\Delta x=0} = \int^{SCCD} d\Gamma\, d\Gamma' \left\{\left[\frac{\partial}{\partial \Delta x}\langle p'_t x'_t|x''\rangle\langle x'|p_t x_t\rangle\right]_{\Delta x=0}/\langle p'_t x'_t|p_t x_t\rangle\right\} \quad (37)$$

where

$$\left[\frac{\partial}{\partial \Delta x}\langle p'_t x'_t|x''\rangle\langle x'|p_t x_t\rangle\right]_{\Delta x=0} = \sqrt{\frac{\gamma}{\pi}}\exp\left[-\gamma\left(\bar{x}-\frac{x_t+x'_t}{2}\right)^2 + \frac{i}{\hbar}(p_t-p'_t)\left(\bar{x}-\frac{x_t+x'_t}{2}\right)\right]\left[\frac{\gamma(x_t-x'_t)}{2}+\frac{i}{2\hbar}(p_t+p'_t)\right]\times \exp\left[-\frac{\gamma(x_t-x'_t)^2}{4}-\frac{i}{2\hbar}(p_t+p'_t)(x_t-x'_t)\right] \quad (38)$$

and

$$\left[\frac{\partial^2}{\partial \Delta x^2}\langle x'|\hat{\delta}_c^{sc}(t;x_c,p_c)|x''\rangle\right]_{\Delta x=0} = \int^{SCCD} d\Gamma\, d\Gamma' \left\{\left[\frac{\partial^2}{\partial \Delta x^2}\langle p'_t x'_t|x''\rangle\langle x'|p_t x_t\rangle\right]_{x=0}/\langle p'_t x'_t|p_t x_t\rangle\right\} \quad (39)$$

where

$$\left[\frac{\partial^2}{\partial \Delta x^2}\langle p'_t x'_t|x''\rangle\langle x'|p_t x_t\rangle\right]_{\Delta x=0} = \sqrt{\frac{\gamma}{\pi}}\exp\left[-\gamma\left(\bar{x}-\frac{x_t+x'_t}{2}\right)^2+\frac{i}{\hbar}(p_t-p'_t)\left(\bar{x}-\frac{x_t+x'_t}{2}\right)\right]\times \left\{\left[\frac{\gamma(x_t-x'_t)}{2}+\frac{i}{2\hbar}(p_t+p'_t)\right]^2-\frac{\gamma}{2}\right\}\times \exp\left[-\frac{\gamma(x_t-x'_t)^2}{4}-\frac{i}{2\hbar}(p_t+p'_t)(x_t-x'_t)\right] \quad (40)$$

where $\bar{x} \equiv (x' + x'')/2$ and $\Delta x \equiv x' - x''$, as before.

Then, the semiclassical expressions of momentum and kinetic energy centroid variables read, with the help of eqs 37−40, as

$$p_c^{sc}(t) = -i\hbar \int d\bar{x}\left[\frac{\partial}{\partial \Delta x}\langle x'|\hat{\delta}_c^{sc}(t;x_c,p_c)|x''\rangle\right]_{\Delta x=0} = -i\hbar\int^{SCCD} d\Gamma\, d\Gamma'\left\{\int d\bar{x}\left[\frac{\partial}{\partial \Delta x}\langle p'_t x'_t|x''\rangle\times \langle x'|p_t x_t\rangle\right]_{\Delta x=0}/\langle p'_t x'_t|p_t x_t\rangle\right\} \quad (41)$$

$$= -i\hbar\int^{SCCD} d\Gamma\, d\Gamma' \left[\frac{\gamma(x_t-x'_t)}{2}+\frac{i}{2\hbar}(p_t+p'_t)\right] \equiv \int^{SCCD} d\Gamma\, d\Gamma'\, p_{sc}(p'_t x'_t p_t x_t) \quad (42)$$

$$T_c^{sc}(t) = -\frac{\hbar^2}{2m}\int d\bar{x}\left[\frac{\partial^2}{\partial \Delta x^2}\langle x'|\hat{\delta}_c^{sc}(t;x_c,p_c)|x''\rangle\right]_{\Delta x=0} = -\frac{\hbar^2}{2m}\int^{SCCD} d\Gamma\, d\Gamma'\left\{\int d\bar{x}\left[\frac{\partial^2}{\partial \Delta x^2}\langle p'_t x'_t|x''\rangle\times \langle x'|p_t x_t\rangle\right]_{\Delta x=0}/\langle p'_t x'_t|p_t x_t\rangle\right\} \quad (43)$$

$$= -\frac{\hbar^2}{2m}\int^{SCCD} d\Gamma\, d\Gamma'\left\{\left[\frac{\gamma(x_t-x'_t)}{2}+\frac{i}{2\hbar}(p_t+p'_t)\right]^2-\frac{\gamma}{2}\right\} \equiv \int^{SCCD} d\Gamma\, d\Gamma'\, T_{sc}(p'_t x'_t p_t x_t) \quad (44)$$

Equations 82 and 85 of ref 15 are used here in the derivation of eqs 41 and 43, respectively. It should be noted that the relationship $T_{sc} = p_{sc}^2/(2m) + \gamma\hbar^2/(4m)$ holds.

III. Results and Discussion

To test the expressions derived in section II, we have calculated the SC-IVR-CD of the TD-QDO, centroid position, momentum, energy, and certain correlation functions for several model potentials. Each centroid quantity calculated from the SC-IVR-CD approach is also compared with those obtained from the CMD approximation. As has been discussed at length before,[14] CMD is not designed, nor is it well-suited, for simulations of nonergodic low-dimensional systems. The CMD results are shown here for illustration of the differences in methods only.

III.A. Preparation of the Initial Centroid Distribution. The initial centroid x_c was sampled from the centroid distribution by using PIMD, while p_c was sampled from a Gaussian distribution, that is,[15]

$$\rho_c(x_c,p_c) = e^{-\beta p_c^2/2m}\rho_c(x_c) \quad (45)$$

The number of discretizations used in the PIMD was from 10 to ~20, depending on convergence. Nose−Hoover chains[22] of length 4 and mass 2 were used in the calculations.

III.B. Local Harmonic Approximation of the Initial QDO. Using path integral molecular dynamics (PIMD) or path integral Monte Carlo (PIMC), one could sample the off-diagonal elements of the QDO from eq 9, which is different from the traditional sampling of the isomorphic ring polymer in PIMD. Off-diagonal variables can be sampled from PIMD simulations or PIMC sampling of open ring polymers. However, using the exact initial QDO for SC-IVR-CD is not always advantageous considering the computational cost. Therefore, a local harmonic approximation may be introduced for the initial QDO.[23] In this approximation, one assumes the initial QDO of eq 15 as

$$\langle x'|\hat{\delta}_c(x_c,p_c)|x''\rangle_\Omega = \sqrt{\frac{m\Omega}{\pi\hbar\alpha}}\exp\left[-\frac{m\Omega\alpha}{4\hbar}(x'-x'')^2+\frac{i}{\hbar}p_c(x'-x'')-\frac{m\Omega}{\hbar\alpha}\left(\frac{x'+x''}{2}-x_c\right)^2\right] \quad (46)$$

where $\alpha \equiv \coth(\Omega\hbar\beta/2) - (2/\Omega\hbar\beta)$. Equation 46 is exact for a harmonic potential, $V(x) = m\Omega^2x^2/2$, and a reasonable approximation to the exact initial QDO for any general potential if the local curvature of the potential is used.[23]

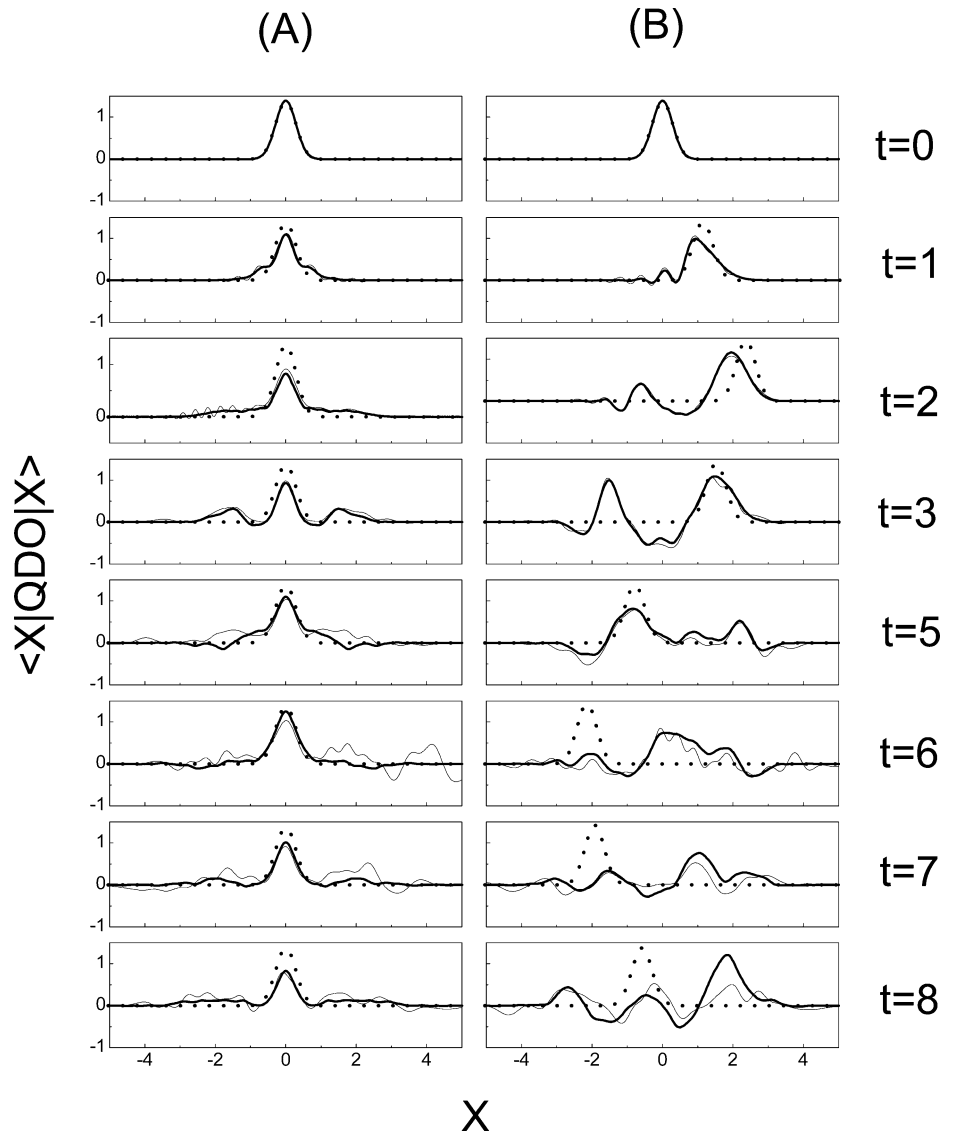

Figure 1. Diagonal elements of the time-dependent QDO for the double-well potential in eq 54: Exact (thick solid line), SC-IVR-CD (thin solid line), and CMD (dotted line); (A) $x_c = 0$, $p_c = 0$ (B) $x_c = 0$, $p_c = 1$. Both exact and CMD calculations use the exact initial QDO, while SC-IVR-CD uses the Gaussian initial QDO [eq 48] which is almost the same as the exact initial QDO.

In the local-curvature approximation of the initial QDO,[23] Ω is replaced by

$$\Omega \rightarrow \Omega_G(x_c) \equiv \sqrt{\frac{1}{m}\frac{\partial^2 V(x)}{\partial x^2}\bigg|_{x=x_c}} \tag{47}$$

in the region of positive curvature and zero in regions of negative curvature. Equation 15 then becomes

$$\langle p_0 x_0|\hat{\delta}_c(x_c,p_c)|p'_0 x'_0\rangle_{\Omega G(x_c)} = \int\int dx'\, dx''\, \langle p_0 x_0|x'\rangle\langle x''|p'_0 x'_0\rangle \sqrt{\frac{m\Omega_G}{\pi\hbar\alpha_G}} \times \exp\left[-\frac{m\Omega_G\alpha_G}{4\hbar}(x'-x'')^2 + \frac{i}{\hbar}p_c(x'-x'') - \frac{m\Omega_G}{\hbar\alpha_G}\left(\frac{x'+x''}{2}-x_c\right)^2\right] \tag{48}$$

where $\Omega_G \equiv \Omega_G(x_c)$ and $\alpha_G \equiv \alpha_G(x_c;\beta) \equiv \coth(\Omega_G(x_c)\hbar\beta/2) - (2/\Omega_G(x_c)\hbar\beta)$. Here, α_G is also defined as zero in the region of nonpositive curvature because $\Omega \rightarrow 0$ for the nonpositive case, and $\alpha_G \rightarrow 0$ as $\Omega \rightarrow 0$. The ratio of Ω/α_G becomes $6/(\beta\hbar)$ in the region of nonpositive curvature. Taking $\sigma_{FG} \equiv 1/\gamma$ as the width of the semiclassical frozen Gaussian wave packet reduces eq 48 to

$$\langle p_0 x_0|\hat{\delta}_c(x_c,p_c)|p'_0 x'_0\rangle_{\Omega_G(x_c)} = \int\int dx'\, dx'' \left\{\sqrt{\frac{m\Omega_G}{\pi\hbar\alpha_G}}\exp\left[-\frac{m\Omega_G\alpha_G}{4\hbar}(x'-x'')^2 + \frac{i}{\hbar}p_c(x'-x'') - \frac{m\Omega_G}{\hbar\alpha_G}\left(\frac{x'+x''}{2}-x_c\right)^2\right]\sqrt{\frac{\gamma}{\pi}} \times \exp\left[-\frac{\gamma}{2}(x'-x_0)^2 - \frac{i}{\hbar}p_0(x'-x_0) - \frac{\gamma}{2}(x''-x'_0)^2 + \frac{i}{\hbar}p'_0(x''-x'_0)\right]\right\} \tag{49}$$

Once the initial QDO is defined, then time propagation of the QDO requires a proper choice of the semiclassical coherent basis set. The details of this topic, possible options for propagation, and the resultant SC-IVR-QDO are mentioned below.

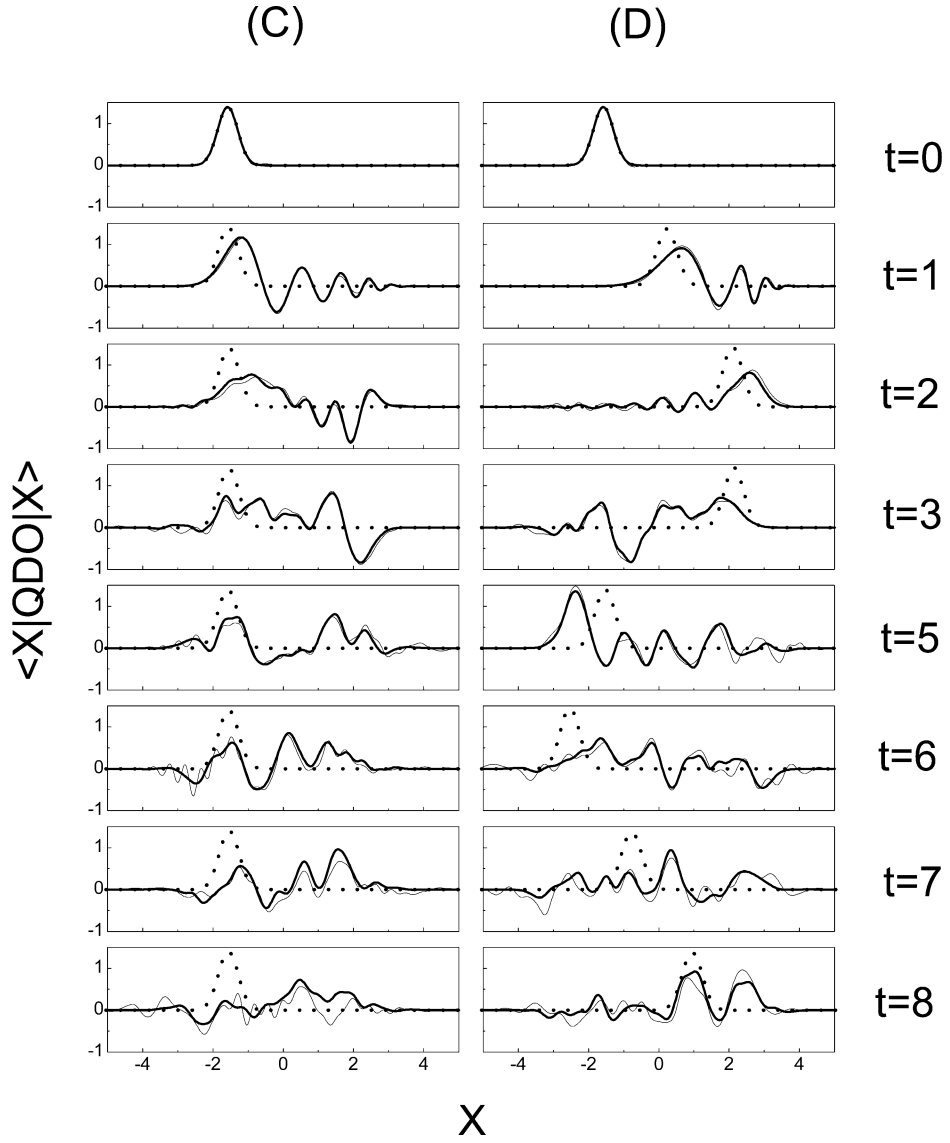

Figure 2. Diagonal elements of the time-dependent QDO for the double-well potential in eq 54: Exact (thick solid line), SC-IVR-CD (thin solid line), and CMD (dotted line); (C) $x_c = -\sqrt{5/2}$, $p_c = 0$ (D) $x_c = -\sqrt{5/2}$, $p_c = 2$. Both exact and CMD calculations use the exact initial QDO, while SC-IVR-CD uses the Gaussian initial QDO [eq 48] which is almost the same as the exact initial QDO.

III.C. The Propagations of the SC-IVR-QDO and the SC-IVR Centroid Variables. To test the accuracy of the SC-IVR-CD approach, the dynamics of certain centroid variables were calculated for the double-well potential in eq 53 below. Natural units $k_B = m = \hbar = 1$ were used in the calculations. Also $\Omega = \beta = \gamma = 1$ was assumed. Four typical initial sets of the centroid variable (x_c,p_c) in the double well were investigated: A(0, 0), B(0, 1), C($-\sqrt{5/2}$, 0), D($-\sqrt{5/2}$, 2).

The exact calculations of the TD-QDO and centroid variables utilized the NMM method.[16] Discretization within the range of $[-6, 6]$ with 400 grid points was carried out. For SC-IVR-CD, the TD-QDO [eq 14], $x_c^{sc}(t)$ [eq 32], $V_c^{sc}(t)$ [eq 33], $p_c^{sc}(t)$ [eq 41], and $T_c^{sc}(t)$ [eq 44] were calculated and the total energy centroid variable was obtained from the following equation:

$$H_c^{sc}(t) = T_c^{sc}(t) + V_c^{sc}(t) \tag{50}$$

A fixed width $\gamma = 1$ was used in the coherent state basis, and averaging over 10^5 trajectories was carried out in the SC-IVR-CD calculations. The CMD results in Figures 1−5 come from propagation of the usual CMD equations[14] with the NMM method applied to calculate the QDO in the CMD approximation [eq 12].

Figure 1A shows that the QDO from any method for these initial conditions does not change its centroid position, but its shape is clearly time-dependent. The approximate CMD QDO fails to reflect this fact because the CMD QDO time dependence is determined by only the centroid position and momentum variables. Figure 1A also reveals that the SC-IVR-CD QDO follows the shape of the exact QDO to a good approximation. In Figure 1B, the CMD QDO initially follows the exact QDO but later deviates from the exact one, while the SC-IVR-CD QDO reproduces the exact QDO reasonably well. The most drastic contrast is seen in Figure 2C where the CMD QDO remains in the minimum of the double well without any noticeable change (these initial conditions have zero initial centroid momentum), while the SC-IVR-CD QDO and the exact QDO evolve from one side to the other side of the double well. This case reveals some degree of quantum tunneling through the barrier of the double well. The quantum tunneling is also

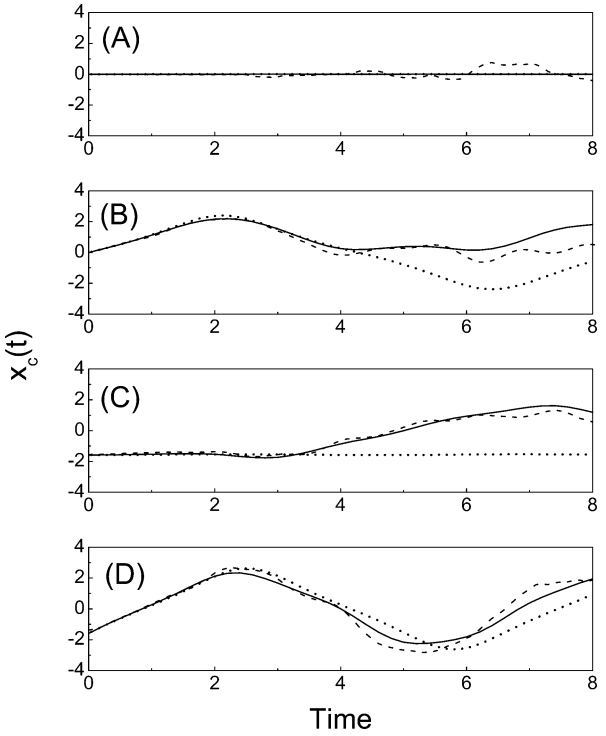

Figure 3. Time-dependent centroid position, $x_c(t)$ for the double-well potential in eq 54: Exact (solid line), SC-IVR-CD (dashed line), and CMD (dotted line), for which the diagonal elements of the time-dependent QDOs have been plotted in Figures 1 and 2: (A) $x_c = 0$, $p_c = 0$; (B) $x_c = 0$, $p_c = 1$; (C) $x_c = -\sqrt{5/2}$, $p_c = 0$; (D) $x_c = -\sqrt{5/2}$, $p_c = 2$.

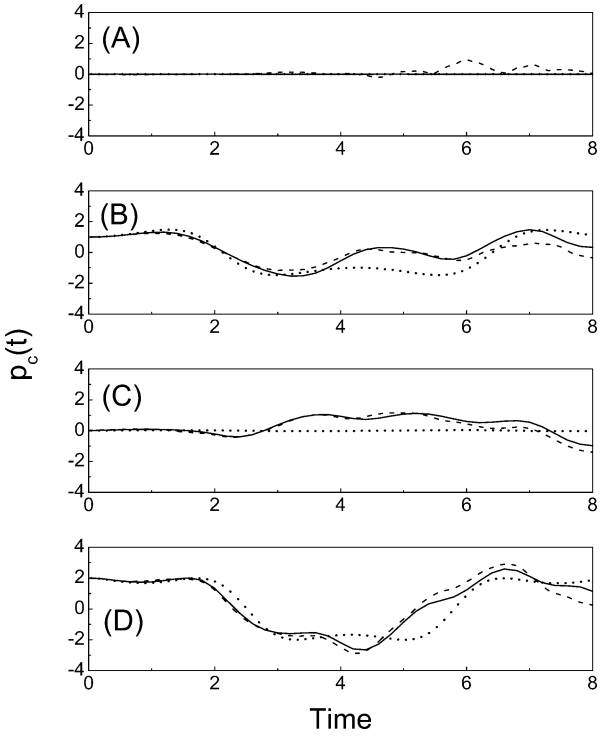

Figure 4. Time-dependent centroid momentum, $p_c(t)$ for the double-well potential in eq 54: Exact (solid line), SC-IVR-CD (dashed line), and CMD (dotted line), for which the diagonal elements of the time-dependent QDOs have been plotted in Figures 1 and 2: (A) $x_c = 0$, $p_c = 0$; (B) $x_c = 0$, $p_c = 1$; (C) $x_c = -\sqrt{5/2}$, $p_c = 0$; (D) $x_c = -\sqrt{5/2}$, $p_c = 2$.

seen in Figure 3C where the time-dependent centroid position variable experiences penetration through the potential barrier.

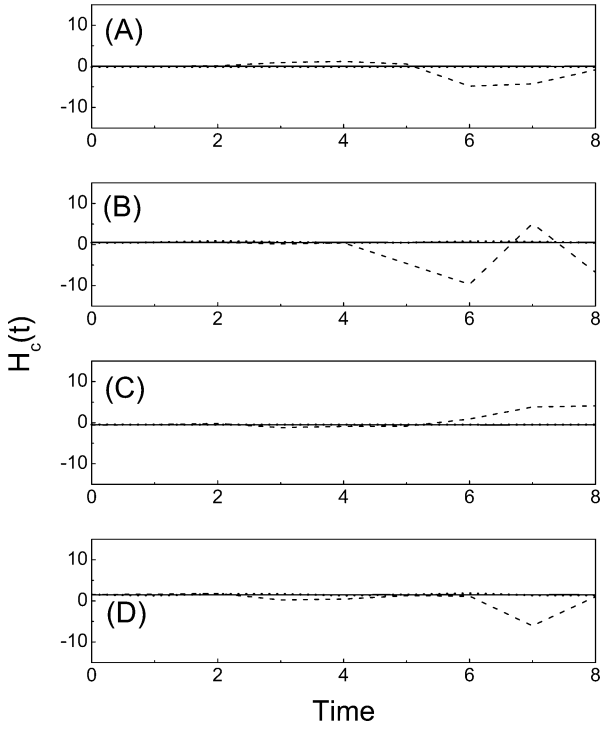

Figure 5. Time-dependent centroid Hamiltonian $H_c(t)$ for the double-well potential in eq 54: Exact (solid line), SC-IVR-CD (dashed line), and CMD (dotted line), for which the diagonal elements of the time-dependent QDOs have been plotted in Figures 1 and 2: (A) $x_c = 0$, $p_c = 0$; (B) $x_c = 0$, $p_c = 1$; (C) $x_c = -\sqrt{5/2}$, $p_c = 0$; (D) $x_c = -\sqrt{5/2}$, $p_c = 2$.

Interestingly, Figures 2D and 3D are cases where CMD acts as a reasonable approximation to the position of the main features of the QDO. This case has an initial condition with the QDO centered in the left well of the double well, but with an initial positive centroid momentum (as opposed to case C). Figures 4 and 5 show that the SC-IVR-CD results are in excellent agreement with the exact ones up to $t = 4$ and then in reasonable agreement beyond that point.

In Figure 5, it is observed that $H_c^{sc}(t)$ of SC-IVR-CD is not as conservative as $H_c(t)$ of CMD. The nonconservative behavior of $H_c^{sc}(t)$ comes from the time-dependent deviation of the SC-IVR-CD QDO from the exact QDO. Neither CMD nor SC-IVR-CD[14,15] gives the exact QDO, but the CMD QDO is conserved exactly, as it must be by definition. Future improvements of the SC-IVR-CD method might seek to better reproduce this conservation property.

III.D. Position−Position Time Correlation Functions. In this section, position−position centroid time correlation functions are calculated and then converted into quantum position autocorrelation functions $C_{xx}(t)$ through eq 2, which is the plotted result. Equation 4 thus becomes

$$C_{xx}^{sc}(t) = \frac{1}{Z}\int\int \frac{dx_c\, dp_c}{2\pi\hbar}\rho_c(x_c,p_c)x_c x_c^{sc}(t) \qquad (51)$$

where

$$x_c^{sc}(t) = \int^{SCCD} d\Gamma\, d\Gamma'\, x_{sc}(p'_t x'_t p_t x_t) \qquad (52)$$

The time-dependent centroid position $x_c^{sc}(t)$ is calculated from SC-IVR-CD. Position−position correlation functions, $C_{xx}^{sc}(t)$, were obtained by averaging over $N_{cent} = 256 \sim 3000$ or more initial centroid points and 10^4 to $\sim 10^5$ semiclassical trajectories

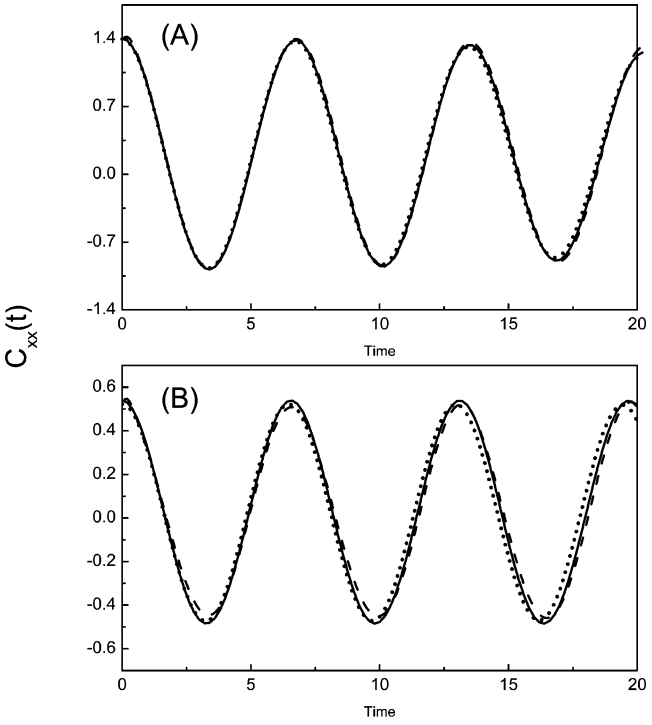

Figure 6. Position time correlation functions for the weak anharmonic potential of eq 53 at two different temperature of (A) $\beta = 1$ and (B) $\beta = 8$: Exact (solid line), SC-IVR-CD (dashed line), and CMD (dotted line).

for the following three model potentials: weak anharmonic, double well, and quartic potentials as described below.

III.D.1 Single-Well Potential with Weak Anharmonicity. The first example was the weakly anharmonic potential:

$$V(x) = \frac{1}{2}x^2 + \frac{1}{10}x^3 + \frac{1}{100}x^4 \tag{53}$$

Figure 6 shows the position−position quantum time correlation function, eq 1, which was converted through eq 2 from the CD position autocorrelation function, eq 51, at two different temperatures. No essential differences between the methods are seen here, especially at $\beta = 1$. Even at the lower temperature, $\beta = 8$, the differences from the exact correlation function are negligible. Therefore, the weakly anharmonic case is very accurately treated by both SC-IVR-CD and CMD.

III.D.2 Double-Well Potential. The electronically adiabatic limit of many chemical reactions can be approximated along the reaction coordinate as a (symmetric or asymmetric) double-well potential. Quantum tunneling effects through the potential barrier are also important for this potential, especially when the temperature is low. Therefore, the coherent motion in a double-well potential serves as one of the most difficult tests for any approximate method. In the present case, a symmetric double well has been chosen, given by

$$V(x) = -\frac{1}{2}x^2 + \frac{1}{10}x^4 \tag{54}$$

Figure 7 reveals that CMD fails to give an accurate correlation function compared to the exact one.[14] CMD gives a reasonable result within short times, up to $t = 4$, but after that it dephases to a plateau value which is not seen in the exact correlation function. SC-IVR-CD gives a significantly better description than does CMD. At temperature $\beta = 1$, it not only has the right short time behavior, but also a qualitatively similar structure at

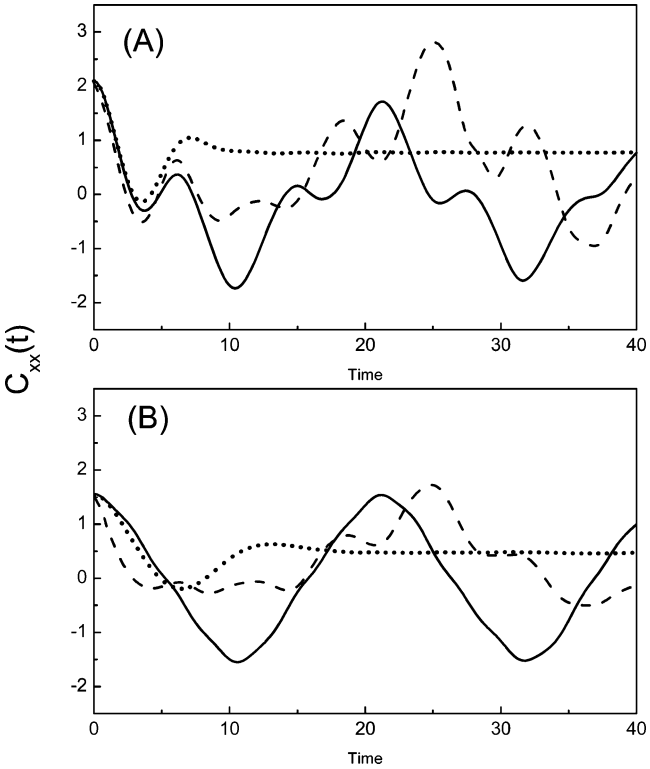

Figure 7. Position time correlation functions for the double-well potential of eq 54 at two different temperature of (A) $\beta = 1$ and (B) $\beta = 8$: Exact (solid line), SC-IVR-CD (dashed line), and CMD (dotted line).

longer times. At a temperature of $\beta = 8$, SC-IVR-CD shows substantial deviation from the exact one at short times, but it still gives some reasonable periodic structure in the longer time limit.

III.D.3 Quartic Potential. A quartic potential is another difficult test for the approximate methods because the anharmonicity of this potential at the equilibrium position is quite large (i.e., there is no quadratic part: even a more realistic potential like the Morse or Lennard-Jones potential can be approximated to be harmonic near the equilibrium position). The quartic potential has the simple functional form

$$V(x) = \frac{1}{4}x^4 \tag{55}$$

For the higher temperature of $\beta = 1$, Figure 8A shows that CMD can provide a good correlation function for short times but does not give a good correlation function after that limit.[14] On the other hand, SC-IVR-CD gives a quite satisfactory result over the entire range. At a temperature of $\beta = 8$, however, a different trend is observed. While SC-IVR-CD remains a reasonably good approximation, CMD becomes an even better case at this temperature. This reinforces the observation that CMD may be a good choice for any potential at very low temperature, a feature of CMD that is well-known.[14]

III.E. Discussion. Before we can draw conclusions about this work, some further discussion is appropriate. One important issue in SC-IVR-CD concerns the local harmonic approximation for the QDO. The initial QDO are obviously not Gaussian; however, the approximation is clearly a convenient choice for SC-IVR-CD sampling. This approximation is obviously reasonable at high temperature, but at lower temperatures the QDO deviates somewhat from a Gaussian shape and especially the width of the initial QDO varies more sensitively as a function

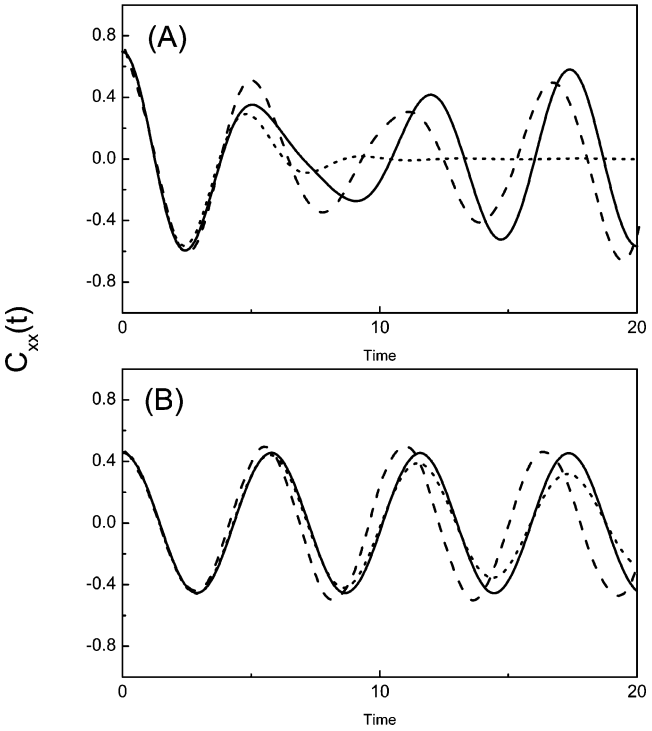

Figure 8. Position time correlation functions for the quartic potential of eq 55 at two different temperature (A) $\beta = 1$ and (B) $\beta = 8$: Exact (solid line), SC-IVR-CD (dashed line), and CMD (dotted line).

of position. On the other hand, the initial approximation for the QDO seems not likely to be the main factor which causes SC-IVR-CD to become inaccurate. Inspection of Figures 1 and 2 shows that the differences between the initial QDO and the QDO at later times is significantly greater than any differences between the two initial QDO representations, so the former features are likely to dominate the deviations between SC-IVR-CD and exact CD.

Based on the discussion in the proceeding paragraph, one can infer that the underlying accuracy of SC-IVR is crucial for the overall accuracy of SC-IVR-CD. Figures 9 and 10 illustrate this point for two calculations which are not directly related to the SC-IVR-CD formalism. By a comparison of Figures 9 and 10 with Figures 6−8, one sees that the onset of inaccuracy in the SC-IVR-CD position correlation functions occurs at, or very nearly at, the same time as inaccuracies occur in the SC-IVR curves in Figures 9 and 10. It should be noted that in Figures 9 and 10 an initial Gaussian wave packet was propagated with no CD formalism (e.g., QDO, centroid TCFs, etc.) being involved in the calculations. The initial Gaussian was defined by position, momentum, and γ: weakly harmonic (1.4, 0, 1), double well (2, 0, $\sqrt{2}$), quartic (1, 0, 1). Each frozen Gaussian basis had the same width as that of the initial Gaussian wave packet.

Another important issue in SC-IVR-CD concerns the sampling. There are two kinds of sampling that are required simultaneously in the current scheme: SC-IVR trajectories, $\{p_0x_0;p'_0x'_0\}$ and centroid initial conditions, $\{p_c,x_c\}$. The former should be large enough, generally 10^4 to $\sim 10^5$, to reach the converged SC-IVR limit, while the latter needs to be large enough to adequately sample the thermal centroid distribution. The resulting computational cost is proportional to their product; $N_{\text{traj}} \times N_{\text{cent}}$. A larger number of SC-IVR trajectories will result in less noisy results at a longer time, while a larger number of centroid initial conditions leads to the correct statistical averages of centroid variables. In addition, some degree of time averaging

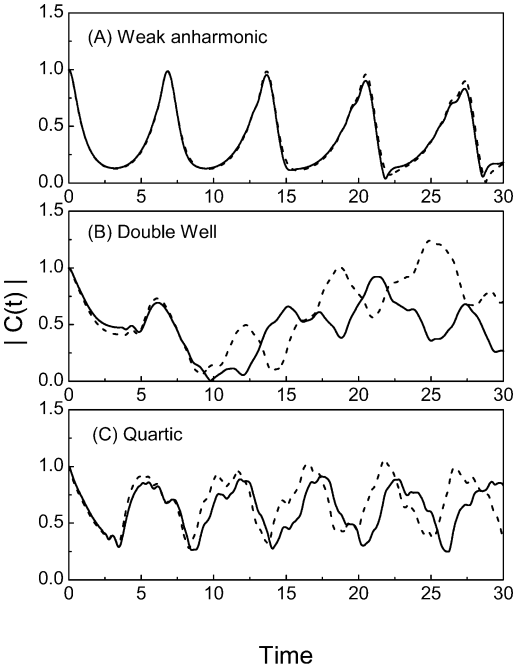

Figure 9. Comparison of the magnitude of the overlap function, $|C(t)| = |\langle\Psi(0)|\Psi(t)\rangle|$ from exact wave packet propagation (by the Split Operator technique[24]) (solid line) and SC-IVR (dashed line). The SC-IVR results were obtained using 10^5 coherent states. A single wave packet was propagated for (a) the weak anharmonic potential, (b) double well, and (c) quartic potential.

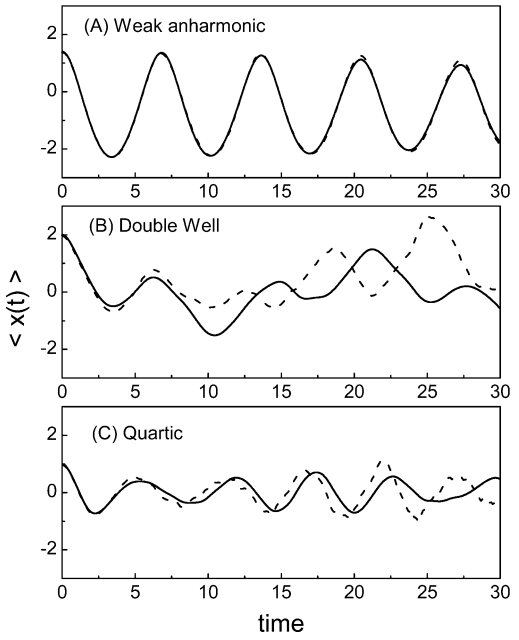

Figure 10. Comparison of average position, $\langle x(t)|\rangle = |\langle\Psi(0)|\Psi(t)\rangle|$ from exact wave packet propagation (by the Split Operator technique[24]) (solid line) and SC-IVR (dashed line). The SC-IVR results were obtained using 10^5 coherent states. A single wave packet was propagated for (a) the weak anharmonic potential, (b) double well, and (c) quartic potential.

is warranted in the calculation of SC-IVR-CD TCFs. However, this must be carried out with care given that the SC-IVR-IVRCD centroid trajectories begin to diverge from the exact results in significant fashion at longer times.

IV. Concluding Remarks

In this paper a SC-IVR implementation of centroid dynamics (SC-IVR-CD) has been introduced and tested for some simple

one-dimensional model potentials. For the case of weak anharmonicity or low temperature, CMD is seen to be as good as or better than SC-IVR-CD. On the other hand, the latter method works better in the case of larger anharmonicity and higher temperatures (albeit at a significant increase in computational cost). SC-IVR-CD, in fact, gives quite good correlation functions for any of the potentials at moderate temperatures. The double-well potential is seen to be the hardest case for SC-IVR-CD, because it cannot give full coherent quantum tunneling behavior. Still SC-IVR-CD can capture a reasonable degree of tunneling and shows a qualitatively similar correlation function to the exact one, whereas CMD simply dephases.

Using full SC-IVR-CD in realistic many-dimensional condensed phase systems does not yet seem feasible given the large degree of required averaging. One possible breakthrough for this problem could be a hybrid method where SC-IVR-CD is used for only a few key degrees of freedom, while the remaining "bath" is treated with a simpler method like CMD (especially in a Gaussian approximation[23]). Further development of the SC-IVR-CD methodology will be the topic of future research.

Acknowledgment. This research was supported by a Grant from the National Science Foundation (CHE-0317132). We thank Dr. Seogjoo Jang, Professor Haobin Wang, and Professor William H. Miller for many helpful discussions. An allocation of computer time from the Center for High Performance Computing at the University of Utah is gratefully acknowledged. The computations were also performed on the National Science Foundation Terascale Computing System at the Pittsburgh Supercomputing Center and at the National Center for Supercomputing Applications at the University of Illinois at Urbana-Champaign, which are funded through the National Science Foundation.

References and Notes

(1) Berne, B. J.; Thirumalai, D. *Annu. Rev. Phys. Chem.* **1986**, *37*, 401.
(2) Miller, W. H. *J. Chem. Phys.* **1970**, *53*, 3578; Miller, W. H.; George, T. F. *J. Chem. Phys.* **1972**, *56*, 5668.
(3) Heller, E. J. *J. Chem. Phys.* **1981**, *75*, 2923.
(4) Kluk, E.; Herman, M. F.; Davis, H. L. *J. Chem. Phys.* **1986**, *84*, 326.
(5) Miller, W. H. *J. Chem. Phys.* **1991**, *95*, 9428.
(6) Kay, K. G. *J. Chem. Phys.* **1994**, *100*, 4377; **1994**, *100*, 4432; **1994**, *101*, 2250.
(7) Grossmann, F.; Xavier A. L., Jr. *Phys. Lett. A.* **1998**, *243*, 243.
(8) Campolieti, G.; Brumer, P. *Phys. Rev. A.* **1994**, *50*, 997.
(9) Thoss, M.; Wang, H.; Miller, W. H. *J. Chem. Phys.* **2001**, *114*, 9220.
(10) Wang, H.; Thoss, M.; Miller, W. H. *J. Chem. Phys.* **2000**, *112*, 47.
(11) Krilov, G.; Sim, E.; Berne, B. J. *J. Chem. Phys.* **2001**, *114*, 1075.
(12) Skilling, J. *Maximum Entropy and Bayesian Methods*; Kluwer: Academic: Dordrecht, 1989.
(13) Cao, J.; Voth, G. A. *J. Chem. Phys.* **1993**, *99*, 10070; **1994**, *100*, 5093; **1994**, *100*, 5106; **1994**, *101*, 6157; **1994**, *101*, 6158.
(14) Jang, S.; Voth, G. A. *J. Chem. Phys.* **1999**, *111*, 2371.
(15) Jang, S.; Voth, G. A. *J. Chem. Phys.* **1999**, *111*, 2357.
(16) Thirumalai, D.; Bruskin, E. J.; Berne, B. J. *J. Chem. Phys.* **1983**, *79*, 5063.
(17) Thompson, K.; Makri, N. *Phys. Rev. E.* **1999**, *59*, R4729.
(18) Shao, J.; Makri, N. *J. Phys. Chem. A.* **1999**, *103*, 7753.
(19) Skinner, D. E.; Miller, W. H. *J. Chem. Phys.* **1999**, *111*, 10787.
(20) Sun, X.; Miller, W. H. *J. Chem. Phys.* **1999**, *110*, 6635.
(21) Herman, M. F.; Kluk, E. *Chem. Phys.* **1984**, *91*, 27.
(22) Jang, S.; Voth, G. A. *J. Chem. Phys.* **1997**, *107*, 9514.
(23) Ka, B. J.; Voth, G. A. Manuscript to be submitted for publication.
(24) Feit, M. D.; Fleck, J. A., Jr.; Steiger, A. *J. Comput. Phys.* **1982**, *47*, 412.